

A renormalizable left-right symmetric model with low scale seesaw mechanisms

A. E. Cárcamo Hernández^{*} and Ivan Schmidt[†]

*Universidad Técnica Federico Santa María and Centro Científico-Tecnológico de Valparaíso,
Casilla 110-V, Valparaíso, Chile*

(Dated: March 27, 2022)

We propose a low scale renormalizable left-right symmetric theory that successfully explains the observed SM fermion mass hierarchy, the tiny values for the light active neutrino masses, the lepton and baryon asymmetries of the Universe, as well as the muon and electron anomalous magnetic moments. In the proposed model the top and exotic quarks obtain masses at tree level, whereas the masses of the bottom, charm and strange quarks, tau and muon leptons are generated from a tree level Universal Seesaw mechanism, thanks to their mixings with the charged exotic vector like fermions. The masses for the first generation SM charged fermions arise from a radiative seesaw mechanism at one loop level, mediated by charged vector like fermions and electrically neutral scalars. The light active neutrino masses are produced from a one-loop level inverse seesaw mechanism. Our model is also consistent with the experimental constraints arising from the Higgs diphoton decay rate. We also discuss the Z' and heavy scalar production at a proton-proton collider.

I. INTRODUCTION

Despite the great success of the Standard Model (SM) as a theory of fundamental interactions, it features drawbacks such as, for example, the lack of explanation of the SM flavor structure; in particular, the observed pattern of SM fermion masses and mixings, the origin of Dark Matter (DM), the source of parity violation in electroweak (EW) interactions, the lepton and baryon asymmetries of the Universe and the anomalous magnetic moments of the muon and electron. In order to address these issues, it is necessary to propose a possible more general higher energy theory. In this sense, left-right symmetric electroweak extensions of the Weinberg-Salam theory have many appealing features, foremost of which is to address the origin of parity violation as a low energy effect, a remnant of its breaking at a certain high energy scale. We are therefore proposing, as a possible explanation of the problems listed before, a minimal renormalizable Left-right symmetric theory [1, 2] based on the gauge symmetry $SU(3)_C \times SU(2)_L \times SU(2)_R \times U(1)_{B-L}$, supplemented by the $Z_4^{(1)} \times Z_4^{(2)}$ discrete group, where the $Z_4^{(1)}$ symmetry is completely broken, whereas the $Z_4^{(2)}$ symmetry is broken down to the preserved Z_2 , thus allowing the implementation of a radiative inverse seesaw mechanism to generate the tiny masses of the light active neutrinos. In fact, left-right models are particularly appealing to consider as extensions of the SM, since they have the possibility of explaining its parity feature at low energy, having a symmetry between left and right particles at higher energies. In the proposed model, the top and exotic quarks obtain masses at tree level whereas the masses of the bottom, charm and strange quarks, tau and muon leptons arise from a tree level Universal Seesaw mechanism. The masses for the first generation SM charged fermions are generated from a one loop level radiative seesaw mechanism mediated by charged vector like fermions and electrically neutral scalars.

Some recent left-right symmetric models have been considered in Refs. [3–6]. Unlike the model of Ref [3], where non renormalizable Yukawa interactions are employed for the implementation of a Froggatt Nielsen mechanism to produce the current SM fermion mass and mixing pattern, our proposed model is a fully renormalizable theory, with minimal particle content and symmetries, where tree level Universal and a one-loop level radiative inverse seesaw mechanisms

^{*}Electronic address: antonio.carcamo@usm.cl

[†]Electronic address: ivan.schmidt@usm.cl

are combined to explain the observed hierarchy of SM fermion masses and fermionic mixing parameters. Furthermore, unlike Ref. [3] our model successfully explains the electron and muon anomalous magnetic moments and includes a discussion about leptogenesis and collider signatures of heavy scalar and Z' gauge bosons, which is not presented in [3]. In our current model, the charged vector-like leptons responsible for the tree level Universal and one-loop level radiative seesaw mechanism that produces the SM charged fermion mass hierarchy, allows to reproduce the measured values of the muon and electron anomalous magnetic moments, thus linking the fermion mass generation mechanism and the $g - 2$ anomalies, which is not given in the left-right symmetric model of Ref. [3]. Moreover, unlike the left-right symmetric theory of Ref. [5], our model does not rely on the inclusion of scalar leptoquarks to generate one loop level masses for the SM charged fermions and light active neutrinos. Besides that, whereas in the left-right symmetric model of [6] the light active neutrino masses are generated from a combination of type I and type II seesaw mechanisms, in our model the tiny masses of the light active neutrinos are produced from an inverse seesaw mechanism at one loop level. Another difference of our model with the one proposed of [6] is that in the former a mechanism for explaining the SM charged fermion mass hierarchy is presented, whereas in the latter such mechanism is not given.

On the other hand, the renormalizable left-right symmetric theory proposed in this paper has a much more economical particle content compared to the left-right symmetric model considered in [4]. For instance, whereas the scalar sector of left-right symmetric model of Ref. [4] has one scalar bidoublet, one $SU(2)_L$ scalar triplet (transforming as a $SU(2)_R$ doublet) and one $SU(2)_R$ scalar triplet (transforming as a $SU(2)_L$ doublet), thus amounting to 32 scalar degrees of freedom, our current left-right model has one scalar bidoublet, one $SU(2)_L$ scalar doublet, one $SU(2)_R$ scalar doublet, two electrically neutral gauge singlet real scalars and two electrically neutral gauge singlet complex scalars, which corresponds to 22 scalar degrees of freedom. Another advantage of our proposal with respect to the one presented in [4] is that in the former a mechanism that naturally explains the SM fermion mass hierarchy is presented, whereas the latter does not include such mechanism.

The paper is organized as follows. In section II we outline the proposed model. The implications of our model in the SM fermion hierarchy is discussed in section III. The consequences of our model in leptogenesis are described in section IV, while the model scalar potential is analyzed in section V. The implications of our model in the Higgs diphoton decay are discussed in section VI, and in section VII we analyze its application to the muon and electron anomalous magnetic moments. The Z' and heavy scalar production at a proton-proton collider are discussed in sections VIII and IX, respectively. We conclude in section X.

II. AN EXTENDED LEFT-RIGHT SYMMETRIC MODEL

Before providing a detailed explanation of our left-right symmetric model, we will explain the reasoning behind introducing extra scalars, fermions and symmetries, needed for implementing an interplay of tree level universal and radiative seesaw mechanism to explain the SM charged fermion mass hierarchy and one loop level inverse seesaw mechanism to generate the tiny neutrino masses. It is worth mentioning that in our proposed model, the mass of the top quark will be generated from a renormalizable Yukawa operator, with an order one Yukawa coupling, i.e.

$$\overline{Q}_{3L} \Phi Q_{iR}, \quad i = 1, 2, 3 \quad (1)$$

where Q_{3L} and Q_{iR} are $SU(2)_L$ and $SU(2)_R$ quark doublets, respectively, whereas Φ is a scalar bidoublet, with the VEV pattern

$$\langle \Phi \rangle = \begin{pmatrix} v_1 & 0 \\ 0 & v_2 \end{pmatrix}, \quad (2)$$

where we have set $v_2 = 0$ to prevent a bottom quark mass arising from the above given Yukawa interaction. Now, to generate tree level masses via a Universal Seesaw mechanism for the bottom, strange and charm quarks, as well as for the tau and muon leptons, one loop level masses for the first generation SM charged fermions and the tiny masses

for the light active neutrinos via a one loop level inverse seesaw mechanism, we need to forbid the operators:

$$\begin{aligned} \overline{Q}_{nL}\Phi Q_{iR}, & \quad \overline{Q}_{nL}\tilde{\Phi}Q_{iR}, & n=1,2, & \quad i=1,2,3, \\ \overline{L}_{iL}\tilde{\Phi}L_{jR}, & \quad \overline{L}_{iL}\tilde{\chi}_L N_{jR}, & (m_N)_{ij}\overline{N}_{iR}N_{jR}^C, & \quad i,j=1,2,3. \end{aligned} \quad (3)$$

and allow the operators:

$$\begin{aligned} \overline{Q}_{3L}\chi_L B_{1R}, & \quad \overline{Q}_{nL}\chi_L B_{2R}, & \overline{B}_{nL}\chi_R^\dagger Q_{iR}, & \quad \overline{B}_{1L}\rho B_{1R}, & \quad \overline{B}_{2L}\sigma B_{2R}, \\ \overline{Q}_{nL}\tilde{\chi}_L T_R, & \quad \overline{T}_L\tilde{\chi}_R^\dagger Q_{iR}, & \overline{T}_L\sigma T_R, & \quad n=1,2, & \quad i=1,2,3, \\ \overline{L}_{iL}\chi_L E_{nR}, & \quad \overline{E}_{nL}\chi_R^\dagger L_{jR}, & \overline{E}_{nL}\eta E_{nR}, & & \\ \overline{L}_{iL}\Phi L_{jR}, & \quad \overline{N}_{iR}^C\tilde{\chi}_R^\dagger L_{jR}, & \overline{\Omega}_{nR}\Omega_{nR}^C\eta, & \quad \overline{N}_{nR}\Omega_{kR}^C\varphi, & \quad n,k=1,2. \end{aligned} \quad (4)$$

This requires to add $Z_4^{(1)}$ and $Z_4^{(2)}$ discrete symmetries, which are spontaneously broken, where the former is completely broken, and the latter is broken down to the preserved Z_2 symmetry. Such remaining conserved Z_2 symmetry allows to implement an inverse seesaw mechanism at one loop level to produce the tiny neutrino masses. Here L_{iL} and L_{iR} are $SU(2)_L$ and $SU(2)_R$ lepton doublets, respectively, while N_{iR} ($i=1,2,3$) and Ω_{nR} ($n=1,2$) are gauge singlet neutral leptons. Let us note that the gauge singlet neutral leptons Ω_{nR} ($n=1,2$) are crucial for generating the term $(m_N)_{ij}\overline{N}_{iR}N_{jR}^C$ ($i,j=1,2,3$) at one loop level, thus allowing the implementation of the one-loop level inverse seesaw mechanism. Additionally, the above mentioned exotic neutral lepton content is the minimal one required to generate the masses for two light active neutrinos, as required from the neutrino oscillation experimental data. Besides that, the SM charged fermion sector has to be extended to include the following heavy fermions: up type quark T , down type quarks B_n and charged leptons E_n ($n=1,2$) in singlet representations under $SU(2)_L \times SU(2)_R$. As a consequence of the above mentioned exotic charged fermion spectrum, the SM charged fermion mass matrices will feature a proportionality between rows and columns, thus implying that the first generation SM charged fermions will be massless at tree level. The one loop level corrections to these matrices will break such proportionality, thus yielding one-loop level masses for the up and down quarks as well as for the electron. Consequently, the aforementioned exotic charged fermion spectrum is the minimal necessary so that no massless charged SM-fermions would appear in the model, provided that one loop level corrections are taken into account.

On the other hand, in what regards the scalar sector, it is worth mentioning that χ_L and χ_R are $SU(2)_L$ and $SU(2)_R$ scalar doublets, respectively, whereas η , σ and φ are gauge singlet scalars. Furthermore, the χ_L (χ_R) scalar is crucial for generating mass mixing terms between left (right) handed SM charged fermions and right (left) handed exotic charged fermions. Furthermore, the $SU(2)_R$ scalar doublet χ_R is crucial for triggering the spontaneous breaking of the $SU(2)_L \times SU(2)_R \times U(1)_{B-L}$ symmetry down to the SM electroweak gauge group. Besides that, the η , σ and φ are gauge singlet scalars, whose inclusion is necessary for generating the masses of the exotic fermions. Moreover, the inclusion of the scalar bidoublet Φ is crucial to generate a tree level top quark mass, as well as the Dirac neutrino submatrix, as will be shown below. The aforementioned scalar content is the minimal required for a successful implementation of the tree level universal and one loop level radiative seesaw mechanisms to explain the SM charged fermion mass hierarchy, as well as of the one loop level inverse seesaw mechanism to produce the tiny neutrino masses. By suitable charge assignments to be specified below, we can implement the aforementioned seesaw mechanisms, useful for explaining the SM fermion mass hierarchy.

Our proposed model is based on the gauge symmetry $SU(3)_C \times SU(2)_L \times SU(2)_R \times U(1)_{B-L}$, supplemented by the

$Z_4^{(1)} \times Z_4^{(2)}$ discrete group, where the full symmetry \mathcal{G} exhibits the following breaking scheme:

$$\begin{aligned}
\mathcal{G} &= SU(3)_C \times SU(2)_L \times SU(2)_R \times U(1)_{B-L} \times Z_4^{(1)} \times Z_4^{(2)} \\
&\Downarrow v_\sigma, v_\eta, v_\rho \\
&SU(3)_C \times SU(2)_L \times SU(2)_R \times U(1)_{B-L} \\
&\Downarrow v_R \\
&SU(3)_C \times SU(2)_L \times U(1)_Y \times Z_2 \\
&\Downarrow v \\
&SU(3)_C \otimes U(1)_Q \times Z_2
\end{aligned} \tag{5}$$

Both $Z_4^{(1)}$ and $Z_4^{(2)}$ discrete groups are spontaneously broken, and are crucial for avoiding a tree level inverse seesaw mechanism. The $Z_4^{(1)}$ symmetry is completely broken, whereas the $Z_4^{(2)}$ symmetry is broken down to the preserved Z_2 symmetry. It is assumed that such discrete symmetries are broken at the scale much larger than the scale of breaking of the left-right symmetry. We further assume that the left-right symmetry breaking scale is about $v_R \sim \mathcal{O}(10)$ TeV. In addition, the $Z_4^{(2)}$ symmetry, which is spontaneously broken to the preserved Z_2 , is crucial in order to forbid the appearance of the term $(m_N)_{ij} \bar{N}_{iR} N_{jR}^C$ at tree level, thus allowing the implementation of the one loop level inverse seesaw mechanism that generates the light active neutrino masses. Besides that, the spontaneously broken $Z_4^{(1)}$ symmetry is crucial to prevent tree level Yukawa mass terms involving the scalar bidoublet and SM charged fermions lighter than the top quark. As we will see in the following, in the SM fermion sector only the top quark will acquire its mass from a renormalizable Yukawa interaction with the scalar bidoublet, whereas the SM charged fermions lighter than the top quark will get their masses from tree level Universal seesaw and radiative seesaw mechanisms.

The fermion assignments under the $SU(3)_C \times SU(2)_L \times SU(2)_R \times U(1)_{B-L}$ group are:

$$\begin{aligned}
Q_{iL} &= \begin{pmatrix} u_{iL} \\ d_{iL} \end{pmatrix} \sim \left(\mathbf{3}, \mathbf{2}, \mathbf{1}, \frac{1}{3} \right), & Q_{iR} &= \begin{pmatrix} \bar{u}_{iR} \\ \bar{d}_{iR} \end{pmatrix} \sim \left(\mathbf{3}, \mathbf{1}, \mathbf{2}, \frac{1}{3} \right), & i &= 1, 2, 3, \\
L_{iL} &= \begin{pmatrix} \nu_{iL} \\ e_{iL} \end{pmatrix} \sim (\mathbf{1}, \mathbf{2}, \mathbf{1}, -1), & L_{iR} &= \begin{pmatrix} \nu_{iR} \\ e_{iR} \end{pmatrix} \sim (\mathbf{1}, \mathbf{1}, \mathbf{2}, -1), & i &= 1, 2, 3, \\
T_R &\sim \left(\mathbf{3}, \mathbf{1}, \mathbf{1}, \frac{4}{3} \right), & T_L &\sim \left(\mathbf{3}, \mathbf{1}, \mathbf{1}, \frac{4}{3} \right), & n &= 1, 2, \\
B_{nR} &\sim \left(\mathbf{3}, \mathbf{1}, \mathbf{1}, -\frac{2}{3} \right), & B_{nL} &\sim \left(\mathbf{3}, \mathbf{1}, \mathbf{1}, -\frac{2}{3} \right), & E_{nR} &\sim (\mathbf{3}, \mathbf{1}, \mathbf{1}, -2), & E_{nL} &\sim (\mathbf{1}, \mathbf{1}, \mathbf{1}, -2), \\
N_{iR} &\sim (\mathbf{1}, \mathbf{1}, \mathbf{1}, 0), & \Omega_{nR} &\sim (\mathbf{1}, \mathbf{1}, \mathbf{1}, 0), & n &= 1, 2.
\end{aligned} \tag{6}$$

Let us note that we have extended the fermion sector of the original left-right symmetric model model by introducing one exotic up type quark T , two exotic down type quarks B_n ($n = 1, 2$), two charged leptons E_n and five Majorana neutrinos, i.e., N_{iR} ($i = 1, 2, 3$) and Ω_{nR} ($n = 1, 2$). Such exotic fermions are assigned as singlet representations of the $SU(2)_L \times SU(2)_R$ group. The above mentioned exotic fermion content is the minimal one required to generate tree level masses via a Universal seesaw mechanism for the bottom, charm and strange quarks, as well as the tau and muon, and one loop level masses for the first generation SM charged fermions, i.e., the up, down quarks, and the electron.

	Q_{nL}	Q_{3L}	Q_{iR}	L_{iL}	L_{iR}	T_L	T_R	B_{nL}	B_{1R}	B_{2R}	E_{nL}	E_{nR}	N_{iR}	Ω_{nR}
$SU(3)_C$	3	3	3	1	1	3	3	3	3	3	1	1	1	1
$SU(2)_L$	2	2	1	2	1	1	1	1	1	1	1	1	1	1
$SU(2)_R$	1	1	2	1	2	1	1	1	1	1	1	1	1	1
$U(1)_{B-L}$	$\frac{1}{3}$	$\frac{1}{3}$	$\frac{1}{3}$	-1	-1	$\frac{4}{3}$	$\frac{4}{3}$	$-\frac{2}{3}$	$-\frac{2}{3}$	$-\frac{2}{3}$	-2	-2	0	0
$Z_4^{(1)}$	-1	i	1	1	- i	1	1	1	- i	1	1	-1	i	- i
$Z_4^{(2)}$	-1	1	1	- i	- i	1	-1	1	-1	-1	- i	- i	i	1

Table I: Fermion assignments under $SU(3)_C \times SU(2)_L \times SU(2)_R \times U(1)_{B-L} \times Z_4^{(1)} \times Z_4^{(2)}$. Here $i = 1, 2, 3$ and $n = 1, 2$

The scalar assignments under the $SU(3)_C \times SU(2)_L \times SU(2)_R \times U(1)_{B-L}$ group are:

$$\begin{aligned}
\Phi &= \begin{pmatrix} \frac{1}{\sqrt{2}}(v_1 + \phi_{1R}^0 + i\phi_{1I}^0) & \phi_2^+ \\ \phi_1^- & \frac{1}{\sqrt{2}}(v_2 + \phi_{2R}^0 + i\phi_{2I}^0) \end{pmatrix} \sim (\mathbf{1}, \mathbf{2}, \mathbf{2}, 0), \\
\chi_L &= \begin{pmatrix} \chi_L^+ \\ \frac{1}{\sqrt{2}}(v_L + \text{Re } \chi_L^0 + i \text{Im } \chi_L^0) \end{pmatrix} \sim (\mathbf{1}, \mathbf{2}, \mathbf{1}, 1), \quad \chi_R = \begin{pmatrix} \chi_R^+ \\ \frac{1}{\sqrt{2}}(v_R + \text{Re } \chi_R^0 + i \text{Im } \chi_R^0) \end{pmatrix} \sim (\mathbf{1}, \mathbf{1}, \mathbf{2}, 1) \\
\sigma &\sim (\mathbf{1}, \mathbf{1}, \mathbf{1}, 0), \quad \varphi \sim (\mathbf{1}, \mathbf{1}, \mathbf{1}, 0), \quad \eta \sim (\mathbf{1}, \mathbf{1}, \mathbf{1}, 0), \quad \rho \sim (\mathbf{1}, \mathbf{1}, \mathbf{1}, 0).
\end{aligned} \tag{7}$$

To implement the tree level Universal and radiative seesaw mechanisms we have introduced the scalars χ_L, χ_R which are responsible for generating tree level mixings between the exotic and SM fermions. We have further introduced the gauge singlet scalars σ and φ which are crucial for the implementation of the radiative inverse seesaw mechanism necessary to produce the light active neutrino masses. Furthermore, the gauge singlet scalar σ provides tree level masses for the exotic T and B_1 quarks. Besides that, the gauge singlet scalars ρ and η are included in the scalar spectrum in order to provide tree level masses for the exotic down type quark B_2 and exotic leptons E_{nR} and Ω_{nR} ($n = 1, 2$), without the need of invoking soft-breaking mass terms. Furthermore, we have also included the scalar bidoublet Φ , which is responsible for generating the top quark mass from the renormalizable Yukawa operator $\bar{Q}_{3L} \Phi Q_{iR}$ ($i = 1, 2, 3$).

The vacuum expectation values (VEVs) of the scalars Φ, χ_L and χ_R are:

$$\langle \Phi \rangle = \begin{pmatrix} v_1 & 0 \\ 0 & v_2 \end{pmatrix}, \quad \langle \chi_L \rangle = \begin{pmatrix} 0 \\ v_L \end{pmatrix}, \quad \langle \chi_R \rangle = \begin{pmatrix} 0 \\ v_R \end{pmatrix}, \tag{8}$$

where for the sake of simplicity we will set $v_2 = 0$.

The fermion assignments under $Z_4^{(1)} \times Z_4^{(2)}$ are:

$$\begin{aligned}
Q_{nL} &\sim (-1, -1), & Q_{3L} &\sim (i, 1), & Q_{jR} &\sim (1, 1), & T_L &\sim (1, 1), & T_R &\sim (1, -1), \\
B_{nL} &\sim (1, 1), & B_{1R} &\sim (-i, -1), & B_{2R} &\sim (1, -1), & L_{jL} &\sim (1, -i), & L_{jR} &\sim (-i, -i), \\
E_{nL} &\sim (1, -i), & E_{nR} &\sim (-1, -i), & N_{jR} &\sim (i, i), & \Omega_{nR} &\sim (-i, 1), & j &= 1, 2, 3, \quad n = 1, 2.
\end{aligned} \tag{9}$$

The scalar fields have the following $Z_4^{(1)} \times Z_4^{(2)}$ assignments:

$$\begin{aligned}
\Phi &\sim (i, 1), & \chi_L &\sim (-1, 1), & \chi_R &\sim (1, 1) \\
\varphi &\sim (1, i), & \sigma &\sim (1, -1), & \eta &\sim (-1, 1), & \rho &\sim (i, -1).
\end{aligned} \tag{10}$$

The fermion and scalar assignments under the $SU(3)_C \times SU(2)_L \times SU(2)_R \times U(1)_{B-L} \times Z_4^{(1)} \times Z_4^{(2)}$ symmetry are shown in Tables I and II, respectively.

Let us note that all scalar fields acquire nonvanishing vacuum expectation values, excepting the scalar singlet φ , whose $Z_4^{(2)}$ charge corresponds to a nontrivial charge under the preserved remnant Z_2 symmetry. Furthermore, due

	Φ	χ_L	χ_R	φ	σ	η	ρ
$SU(3)_C$	1	1	1	1	1	1	1
$SU(2)_L$	2	2	1	1	1	1	1
$SU(2)_R$	2	1	2	1	1	1	1
$U(1)_{B-L}$	0	1	1	0	0	0	0
$Z_4^{(1)}$	i	-1	1	1	1	-1	i
$Z_4^{(2)}$	1	1	1	i	-1	1	-1

Table II: Scalar assignments under $SU(3)_C \times SU(2)_L \times SU(2)_R \times U(1)_{B-L} \times Z_4^{(1)} \times Z_4^{(2)}$.

to such remnant Z_2 symmetry, the real and imaginary components of the scalar singlet φ will not have mixings with the remaining CP even and CP odd neutral scalar fields of the model, and thus $\text{Re } \varphi$ and $\text{Im } \varphi$ can be considered as physical fields.

It is worth mentioning that the preserved Z_2 symmetry allows for stable scalar and fermionic dark matter candidates. The scalar dark matter candidate is the lightest among the CP-even and CP-odd neutral components of the gauge singlet scalar φ . The fermionic dark matter candidate is the lightest among the right handed Majorana neutrinos N_{iR} ($i = 1, 2, 3$). In the scenario of a scalar DM candidate, it annihilates mainly into WW , ZZ , $t\bar{t}$, $b\bar{b}$ and $h_{SM}h_{SM}$ via a Higgs portal scalar interaction. These annihilation channels will contribute to the DM relic density, which can be accommodated for appropriate values of the scalar DM mass and of the coupling of the Higgs portal scalar interaction. Some studies of the dark matter constraints for the scenario of scalar singlet dark matter candidate are provided in [7–9]. Thus, for the DM direct detection prospects, the scalar DM candidate would scatter off a nuclear target in a detector via Higgs boson exchange in the t -channel, giving rise to a constraint on the Higgs portal scalar interaction coupling. Regarding the scenario of fermionic DM candidate, the Dark matter relic abundance can be obtained through freeze-in, as shown in [8]. The resulting constraints can therefore be fulfilled for an appropriate region of parameter space, along similar lines of Refs. [8, 10, 11]. A detailed study of the implications of our model in dark matter is beyond the scope of this work and will be done elsewhere.

With the above particle content, the following relevant Yukawa terms arise:

$$\begin{aligned}
-\mathcal{L}_Y = & \sum_{i=1}^3 \alpha_i \bar{Q}_{3L} \Phi Q_{iR} + \sum_{n=1}^2 x_n^{(T)} \bar{Q}_{nL} \tilde{\chi}_L T_R + \sum_{i=1}^3 z_i^{(T)} \bar{T}_L \tilde{\chi}_R^\dagger Q_{iR} \\
& + x_3^{(B)} \bar{Q}_{3L} \chi_L B_{1R} + \sum_{n=1}^2 x_{n2}^{(B)} \bar{Q}_{nL} \chi_L B_{2R} + \sum_{n=1}^2 \sum_{i=1}^3 z_{ni}^{(B)} \bar{B}_{nL} \chi_R^\dagger Q_{iR} \\
& + y_T \bar{T}_L \sigma T_R + y_{B_1} \bar{B}_{1L} \rho B_{1R} + y_{B_2} \bar{B}_{2L} \sigma B_{2R} + \sum_{n=1}^2 y_{E_n} \bar{E}_{nL} \eta E_{nR} \\
& + \sum_{i=1}^3 \sum_{n=1}^2 x_{in}^{(E)} \bar{L}_{iL} \chi_L E_{nR} + \sum_{n=1}^2 \sum_{i=1}^3 z_{nj}^{(E)} \bar{E}_{nL} \chi_R^\dagger L_{jR} \\
& + \sum_{i=1}^3 \sum_{j=1}^3 y_{ij}^{(L)} \bar{L}_{iL} \Phi L_{jR} + \sum_{i=1}^3 \sum_{j=1}^3 x_{ij}^{(N)} \bar{N}_{iR}^C \tilde{\chi}_R^\dagger L_{jR} \\
& + \sum_{n=1}^2 (y_\Omega)_n \bar{\Omega}_{nR} \Omega_{nR}^C \eta + \sum_{n=1}^2 \sum_{k=1}^2 x_{nk}^{(S)} \bar{N}_{nR} \Omega_{kR}^C \varphi + H.c., \tag{11}
\end{aligned}$$

To close this section, in the following we discuss the implications of our model for flavor changing neutral currents (FCNC). The FCNC in the down type quark sector are expected to be very suppressed since at energies below the scale v_R of breaking of the left-right symmetry, only the $SU(2)_L$ scalar doublet χ_L will appear in the down

type quark Yukawa terms. In what regards the up type quark sector, there would be FCNC at tree level, since at low energies (below v_R), the bidoublet scalar Φ and the $SU(2)_L$ scalar doublet χ_L participate in the up type quark Yukawa interactions. However, such FCNC can be suppressed by sufficiently small values of the α_1 and α_2 Yukawa couplings. In particular, setting $\alpha_1 = \alpha_2 = 0$ do not generate problems for the quark masses and mixing parameters. Furthermore, concerning the charged lepton sector, the corresponding FCNC can be suppressed by making the matrix $y_{ij}^{(L)}$ diagonal.

III. FERMION MASS MATRICES.

From the Yukawa interactions, we find that the mass matrices for SM charged fermions are given by:

$$\begin{aligned} M_U &= \begin{pmatrix} \Delta_U & 0_{2 \times 1} & A_U \\ 0_{1 \times 2} & m_t & 0 \\ B_U & 0 & m_T \end{pmatrix}, & A_U &= \begin{pmatrix} x_1^{(T)} \\ x_2^{(T)} \end{pmatrix} \frac{v_L}{\sqrt{2}}, \\ B_U &= \begin{pmatrix} z_1^{(T)} & z_2^{(T)} \end{pmatrix} \frac{v_R}{\sqrt{2}}, & m_t &= x_3^{(Q)} \frac{v_1}{\sqrt{2}}, \end{aligned} \quad (12)$$

$$\begin{aligned} M_D &= \begin{pmatrix} \Delta_D & A_D \\ B_D & M_B \end{pmatrix}, & A_D &= \begin{pmatrix} 0 & x_{12}^{(B)} \\ 0 & x_{22}^{(B)} \\ x_3^{(B)} & x_{32}^{(B)} \end{pmatrix} \frac{v_L}{\sqrt{2}}, \\ B_D &= \begin{pmatrix} z_{11}^{(B)} & z_{12}^{(B)} & z_{13}^{(B)} \\ z_{21}^{(B)} & z_{22}^{(B)} & z_{23}^{(B)} \end{pmatrix} \frac{v_R}{\sqrt{2}}, & M_B &= \begin{pmatrix} m_{B_1} & 0 \\ 0 & m_{B_2} \end{pmatrix}, \end{aligned} \quad (13)$$

$$\begin{aligned} M_E &= \begin{pmatrix} \Delta_E & A_E \\ B_E & C_E \end{pmatrix}, & A_E &= \begin{pmatrix} x_{11}^{(E)} & x_{12}^{(E)} \\ x_{21}^{(E)} & x_{22}^{(E)} \\ x_{31}^{(E)} & x_{32}^{(E)} \end{pmatrix} \frac{v_L}{\sqrt{2}}, \\ B_D &= \begin{pmatrix} z_{11}^{(E)} & z_{12}^{(E)} & z_{13}^{(E)} \\ z_{21}^{(E)} & z_{22}^{(E)} & z_{23}^{(E)} \end{pmatrix} \frac{v_R}{\sqrt{2}}, & C_E &= \begin{pmatrix} m_{E_1} & 0 \\ 0 & m_{E_2} \end{pmatrix}, \end{aligned} \quad (14)$$

As seen from Eqs. (12), (13) and (14), the exotic heavy vector-like fermions mix with the SM fermions lighter than top quark. The masses of these vector-like fermions are much larger than the scale of breaking of the left-right symmetry $v_R \sim \mathcal{O}(10)$ TeV, since the gauge singlet scalars η , σ and ρ are assumed to acquire vacuum expectation values much larger than this scale. Therefore, the charm, bottom and strange quarks, as well as the tau and muon leptons, acquire their masses from the tree-level Universal seesaw mechanism, whereas the first generation SM charged fermions, i.e., the up, down quarks and the electron get one-loop level masses from a radiative seesaw mechanism. Thus, the SM charged fermion mass matrices take the form:

$$\widetilde{M}_U = \begin{pmatrix} \Delta_U + A_U M_T^{-1} B_U & 0_{2 \times 1} \\ 0_{1 \times 2} & m_t \end{pmatrix}, \quad (15)$$

$$\widetilde{M}_D = \Delta_D + A_D M_B^{-1} B_D, \quad (16)$$

$$\widetilde{M}_E = \Delta_E + A_E M_E^{-1} B_E, \quad (17)$$

where Δ_U , Δ_D and Δ_E are the one loop level contributions to the SM charged fermion mass matrices arising from the one-loop Feynman diagrams of Figure 1.

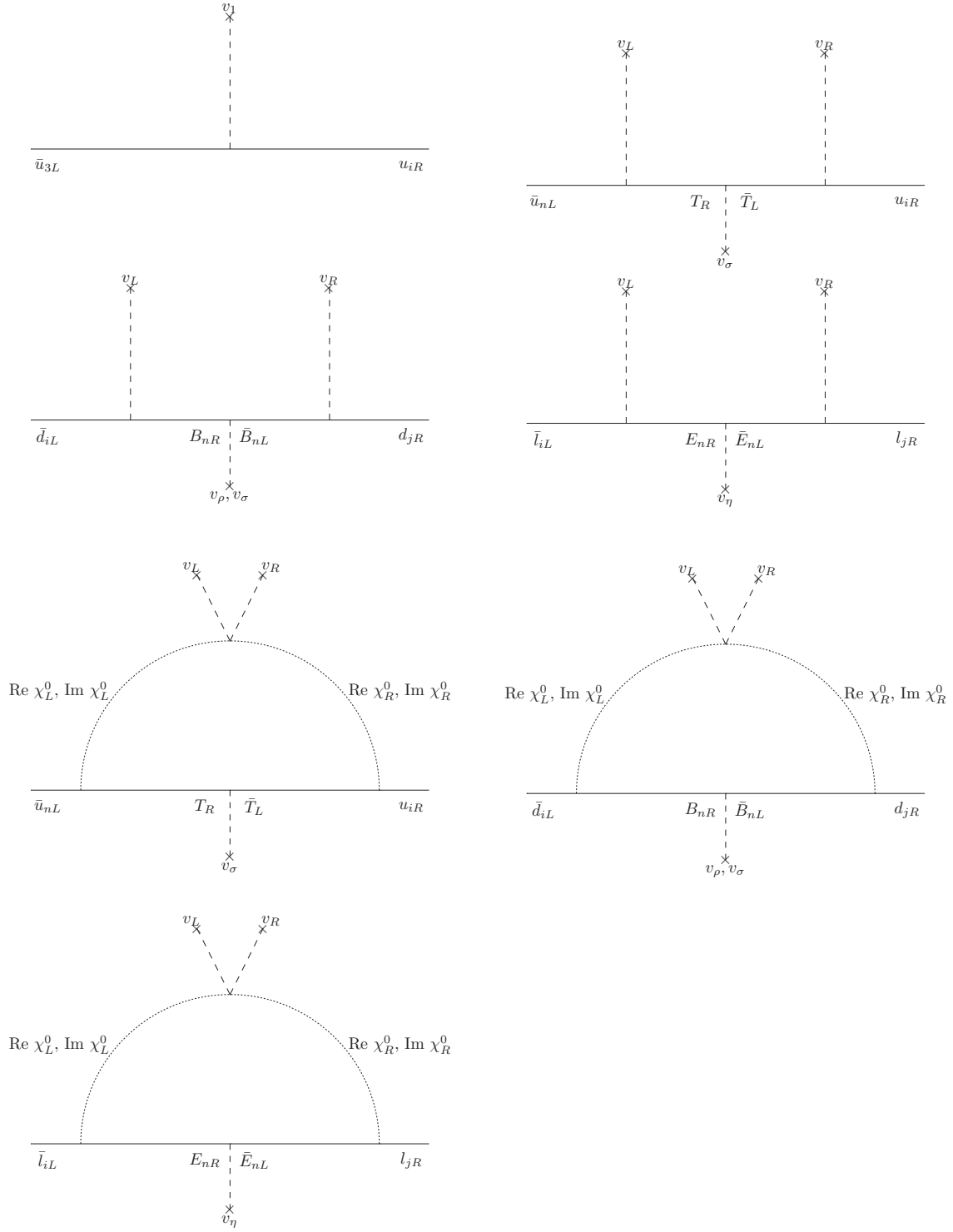


Figure 1: Feynman diagrams contributing to the entries of the SM charged fermion mass matrices. Here, $n = 1, 2$ and $i, j = 1, 2, 3$.

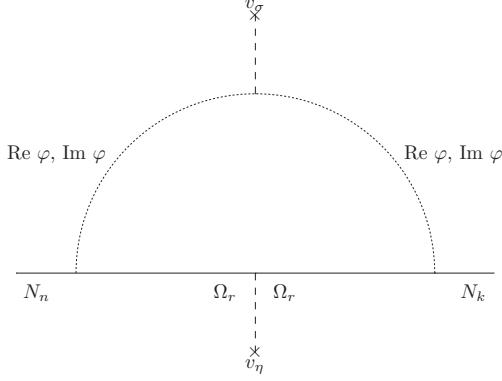


Figure 2: One-loop Feynman diagram contributing to the Majorana neutrino mass submatrix μ . Here, $n, k = 1, 2, 3$ and $r = 1, 2$.

Concerning the neutrino sector, we find that the neutrino Yukawa interactions give rise to the following neutrino mass terms:

$$-\mathcal{L}_{mass}^{(\nu)} = \frac{1}{2} \left(\overline{\nu_L^C} \quad \overline{\nu_R} \quad \overline{N_R} \right) M_\nu \begin{pmatrix} \nu_L \\ \nu_R^C \\ N_R^C \end{pmatrix} + \sum_{n=1}^2 (m_\Omega)_n \overline{\Omega}_{nR} \Omega_{nR}^C + H.c, \quad (18)$$

where the neutrino mass matrix reads:

$$M_\nu = \begin{pmatrix} 0_{3 \times 3} & m_{\nu D} & 0 \\ m_{\nu D}^T & 0 & M \\ 0 & M & \mu \end{pmatrix}, \quad (19)$$

and the submatrices are given by:

$$\begin{aligned} (m_{\nu D})_{ij} &= y_{ij}^{(L)} \frac{v_1}{\sqrt{2}}, & M_{ij} &= x_{ij}^{(N)} \frac{v_R}{\sqrt{2}}, & i, j &= 1, 2, 3, & n, k, r &= 1, 2, \\ \mu_{nk} &= \sum_{r=1}^2 \frac{x_{nr}^{(S)} x_{kr}^{(S)} m_{\Omega_r}^2}{16\pi^2} \left[\frac{m_{\varphi_R}^2}{m_{\varphi_R}^2 - m_{\Omega_r}^2} \ln \left(\frac{m_{\varphi_R}^2}{m_{\Omega_r}^2} \right) - \frac{m_{\varphi_I}^2}{m_{\varphi_I}^2 - m_{\Omega_r}^2} \ln \left(\frac{m_{\varphi_I}^2}{m_{\Omega_r}^2} \right) \right], & & & & & \end{aligned} \quad (20)$$

The μ block is generated at one loop level due to the exchange of Ω_{rR} ($r = 1, 2$) and φ in the internal lines, as shown in Figure 2. To close the corresponding one loop diagram, the following trilinear scalar interaction is needed:

$$V_\mu = A (\varphi^*)^2 \sigma, \quad (21)$$

The light active masses arise from a combination of inverse and linear seesaw mechanisms and the physical neutrino mass matrices are:

$$\widetilde{\mathbf{M}}_\nu = m_{\nu D} (M^T)^{-1} \mu M^{-1} m_{\nu D}^T, \quad (22)$$

$$\mathbf{M}_\nu^{(1)} = -\frac{1}{2} (M + M^T) + \frac{1}{2} \mu, \quad (23)$$

$$\mathbf{M}_\nu^{(2)} = \frac{1}{2} (M + M^T) + \frac{1}{2} \mu. \quad (24)$$

where $M_\nu^{(1)}$ corresponds to the mass matrix for light active neutrinos (ν_a), whereas $M_\nu^{(2)}$ and $M_\nu^{(3)}$ are the mass matrices for sterile neutrinos (N_a^-, N_a^+) which are superpositions of mostly ν_{aR} and N_{aR} as $N_a^\pm \sim \frac{1}{\sqrt{2}} (\nu_{aR} \mp N_{aR})$.

In the limit $\mu \rightarrow 0$, which corresponds to unbroken lepton number, the light active neutrinos become massless. The smallness of the μ - parameter is responsible for a small mass splitting between the three pairs of sterile neutrinos, thus implying that the sterile neutrinos form pseudo-Dirac pairs. The full neutrino mass matrix given by Eq. (19) can be diagonalized by the following rotation matrix [12]:

$$\mathbb{R} = \begin{pmatrix} \mathbf{R}_\nu & \mathbf{R}_1 \mathbf{R}_M^{(1)} & \mathbf{R}_2 \mathbf{R}_M^{(2)} \\ -\frac{(\mathbf{R}_1^\dagger + \mathbf{R}_2^\dagger)}{\sqrt{2}} \mathbf{R}_\nu & \frac{(1-\mathbf{S})}{\sqrt{2}} \mathbf{R}_M^{(1)} & \frac{(1+\mathbf{S})}{\sqrt{2}} \mathbf{R}_M^{(2)} \\ -\frac{(\mathbf{R}_1^\dagger - \mathbf{R}_2^\dagger)}{\sqrt{2}} \mathbf{R}_\nu & \frac{(-1-\mathbf{S})}{\sqrt{2}} \mathbf{R}_M^{(1)} & \frac{(1-\mathbf{S})}{\sqrt{2}} \mathbf{R}_M^{(2)} \end{pmatrix}, \quad (25)$$

where

$$\mathbf{S} = -\frac{1}{4} M^{-1} \mu, \quad \mathbf{R}_1 \simeq \mathbf{R}_2 \simeq \frac{1}{\sqrt{2}} m_{\nu D}^* M^{-1}. \quad (26)$$

Notice that the physical neutrino spectrum is composed of three light active neutrinos and six exotic neutrinos. The exotic neutrinos are pseudo-Dirac, with masses $\sim \pm \frac{1}{2} (M + M^T)$ and a small splitting μ . Furthermore, \mathbf{R}_ν , $\mathbf{R}_M^{(1)}$ and $\mathbf{R}_M^{(2)}$ are the rotation matrices which diagonalize $\widetilde{\mathbf{M}}_\nu$, $\mathbf{M}_\nu^{(1)}$ and $\mathbf{M}_\nu^{(2)}$, respectively.

On the other hand, using Eq. (25) we find that the neutrino fields $\nu_L = (\nu_{1L}, \nu_{2L}, \nu_{3L})^T$, $\nu_R^C = (\nu_{1R}^C, \nu_{2R}^C, \nu_{3R}^C)$ and $N_R^C = (N_{1R}^C, N_{2R}^C, N_{3R}^C)$ are related with the physical neutrino fields by the following relations:

$$\begin{pmatrix} \nu_L \\ \nu_R^C \\ N_R^C \end{pmatrix} = \mathbb{R} \Omega_L \simeq \begin{pmatrix} \mathbf{R}_\nu & \mathbf{R}_1 \mathbf{R}_M^{(1)} & \mathbf{R}_2 \mathbf{R}_M^{(2)} \\ -\frac{(\mathbf{R}_1^\dagger + \mathbf{R}_2^\dagger)}{\sqrt{2}} \mathbf{R}_\nu & \frac{(1-\mathbf{S})}{\sqrt{2}} \mathbf{R}_M^{(1)} & \frac{(1+\mathbf{S})}{\sqrt{2}} \mathbf{R}_M^{(2)} \\ -\frac{(\mathbf{R}_1^\dagger - \mathbf{R}_2^\dagger)}{\sqrt{2}} \mathbf{R}_\nu & \frac{(-1-\mathbf{S})}{\sqrt{2}} \mathbf{R}_M^{(1)} & \frac{(1-\mathbf{S})}{\sqrt{2}} \mathbf{R}_M^{(2)} \end{pmatrix} \begin{pmatrix} \Psi_L^{(1)} \\ \Psi_L^{(2)} \\ \Psi_L^{(3)} \end{pmatrix}, \quad \Psi_L = \begin{pmatrix} \Psi_L^{(1)} \\ \Psi_L^{(2)} \\ \Psi_L^{(3)} \end{pmatrix}, \quad (27)$$

where $\Psi_{jL}^{(1)}, \Psi_{jL}^{(2)} = N_j^+$ and $\Psi_{jL}^{(3)} = N_j^-$ ($j = 1, 2, 3$) are the three active neutrinos and six exotic neutrinos, respectively.

IV. LEPTOGENESIS

In this section we will analyze the implications of our model in leptogenesis. To simplify our analysis we assume that $y^{(L)}$ and $x^{(N)}$ are diagonal matrices and we consider the case where $|y_{11}^{(L)}| \ll |y_{22}^{(L)}|, |y_{33}^{(L)}|$ and $|x_{11}^{(N)}| \ll |x_{22}^{(N)}|, |x_{33}^{(N)}|$. It is worth mentioning that the scenario of diagonal $y^{(L)}$ matrix is crucial for suppressing tree level FCNC in the charged lepton sector. In the above mentioned scenario only the first generation of N_a^\pm can give the contribution to the Baryon asymmetry of the Universe (BAU). We further assume that the exotic leptonic fields E_{nR} and Ω_{nR} are heavier than the lightest pseudo-Dirac fermions $N_1^\pm = N^\pm$, while in addition, for the sake of simplicity, we work in the basis where the SM charged lepton mass matrix is diagonal. Then, the lepton asymmetry parameter, which is induced by decay process of N^\pm , has the following form [13, 14]:

$$\varepsilon_\pm = \frac{\sum_{i=1}^3 [\Gamma(N_\pm \rightarrow \nu_i A_1^0) - \Gamma(N_\pm \rightarrow \nu_i A_1^0)]}{\sum_{i=1}^3 [\Gamma(N_\pm \rightarrow \nu_i A_1^0) + \Gamma(N_\pm \rightarrow \nu_i A_1^0)]} \simeq \frac{\text{Im} \left\{ \left([(y_{N_+})^\dagger (y_{N_-})]^2 \right)_{11} \right\}}{8\pi A_\pm} \frac{r}{r^2 + \frac{\Gamma_\pm}{m_{N_\pm}}}, \quad (28)$$

with:

$$\begin{aligned} r &= \frac{m_{N_+}^2 - m_{N_-}^2}{m_{N_+} m_{N_-}}, & A_\pm &= \left[(y_{N_\pm})^\dagger y_{N_\pm} \right]_{11}, & \Gamma_\pm &= \frac{A_\pm m_{N_\pm}}{8\pi}, \\ y_{N_\pm} &= \frac{y^{(L)}}{\sqrt{2}} (1 \mp S) = \frac{y^{(L)}}{\sqrt{2}} \left(1 \pm \frac{1}{4} M^{-1} \mu \right) \end{aligned} \quad (29)$$

It is worth mentioning that CP violation in the lepton sector necessary to generate the lepton asymmetry parameter, and can arise from complex entries in $y^{(L)}$, M or μ , as indicated by Eqs. (28) and (29).

If one neglects the interference terms involving the two different sterile neutrinos N^\pm , the washout parameter $K_{N^+} + K_{N^-}$ is huge as mentioned in [15]. However, the small mass splitting between the pseudo-Dirac neutrinos leads to a destructive interference in the scattering process [16]. The washout parameter including the interference term is given as follows:

$$K^{eff} \simeq (K_{N^+} \delta_+^2 + K_{N^-} \delta_-^2), \quad (30)$$

where:

$$\delta_\pm = \frac{m_{N^+} - m_{N^-}}{\Gamma_{N^\pm}}, \quad K_{N^\pm} = \frac{\Gamma_\pm}{H(T)}, \quad H(T) = \sqrt{\frac{4\pi^3 g^*}{45}} \frac{T^2}{M_P} \quad (31)$$

where $g^* = 118$ is the number of effective relativistic degrees of freedom, $M_{Pl} = 1.2 \times 10^9$ GeV is the Planck constant and $T = m_{N^\pm}$. In the weak and strong washout regimes, the baryon asymmetry is related to the lepton asymmetry [14] as follows

$$Y_{\Delta B} = \frac{n_B - \bar{n}_B}{s} = -\frac{28}{79} \frac{\epsilon_+ + \epsilon_-}{g^*}, \quad \text{for } K^{eff} \ll 1, \quad (32)$$

$$Y_{\Delta B} = \frac{n_B - \bar{n}_B}{s} = -\frac{28}{79} \frac{0.3(\epsilon_+ + \epsilon_-)}{g^* K^{eff} (\ln K^{eff})^{0.6}}, \quad \text{for } K^{eff} \gg 1, \quad (33)$$

The correlation of the baryon asymmetry parameter Y_B with the leptonic CP violating phase $\delta_{CP}^{(l)}$ for the weak and strong washout regimes is shown in the left and right panels of Figure 3, respectively. The leptonic CP violating phase $\delta_{CP}^{(l)}$ is defined as follows:

$$\delta_{CP}^{(l)} = \arcsin \left(\frac{8\mathcal{J}_{CP}^{(l)}}{\sin 2\theta_{12} \sin 2\theta_{23} \sin 2\theta_{13} \cos \theta_{13}} \right), \quad (34)$$

where $\mathcal{J}_{CP}^{(l)}$ is the Jarlskog invariant of the lepton sector, defined as follows

$$\mathcal{J}_{CP}^{(l)} = \text{Im} [U_{23} U_{13}^* U_{12} U_{22}^*], \quad (35)$$

where \mathbf{U} is the PMNS leptonic mixing matrix given by $\mathbf{U} = \mathbf{R}_\ell^\dagger \mathbf{R}_\nu$, being \mathbf{R}_ℓ and \mathbf{R}_ν the rotation matrices that diagonalize the mass matrices for the SM charged leptons and light active neutrinos, respectively. As shown from the above given relations, phases in the Majorana neutrino mass terms leading to complex entries in the μ block will generate complex entries in the PMNS leptonic mixing matrix, thus yielding a nonvanishing leptonic CP phase $\delta_{CP}^{(l)}$. As shown in Figure 3, our model successfully accommodates the experimental value of the baryon asymmetry parameter Y_B :

$$Y_{\Delta B} = (0.87 \pm 0.01) \times 10^{-10} \quad (36)$$

V. THE SIMPLIFIED SCALAR POTENTIAL

In order to simplify our analysis, we will consider a benchmark scenario where the singlet real scalar fields σ , η and ρ will not feature mixings with the neutral components of the Φ , χ_L and χ_R scalars. The justification of this benchmark scenario arises from the fact that such gauge singlet scalars σ , η and ρ are assumed to acquire vacuum expectation values much larger than the scale of breaking of the left-right symmetry, thus allowing to neglect the mixings of these fields with the Φ , χ_L and χ_R scalars and to treat their scalar potentials independently. Let us note that the mixing angles between those fields are suppressed by the ratios of their VEVs, as follows from the method of recursive

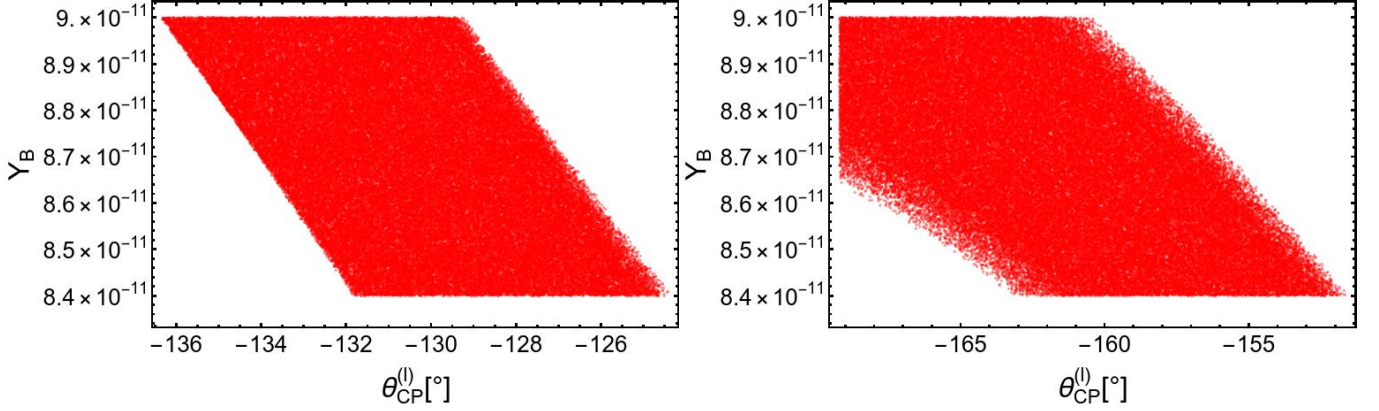


Figure 3: Correlation of the baryon asymmetry parameter Y_B with the leptonic CP violating phase $\delta_{CP}^{(l)}$ for the weak (left-plot) and strong (right-plot) washout regimes.

expansion of Ref. [17]. Furthermore, the preserved remnant Z_2 symmetry will forbid mixings of the $\text{Re } \varphi$ and $\text{Im } \varphi$ scalars with the remaining scalar fields of our model. The scalar potential for the Φ , χ_L and χ_R scalars takes the form:

$$\begin{aligned}
 V = & \mu_1^2(\chi_L^\dagger \chi_L) + \mu_2^2(\chi_R^\dagger \chi_R) + \mu_3^2 \text{Tr}(\Phi^\dagger \Phi) + \mu^2 \text{Tr}(\tilde{\Phi} \Phi^\dagger + \tilde{\Phi}^\dagger \Phi) + \lambda_1(\chi_L^\dagger \chi_L)^2 + \lambda_2(\chi_R^\dagger \chi_R)^2 + \lambda_3(\chi_L^\dagger \chi_L)(\chi_R^\dagger \chi_R) \\
 & + \lambda_4 [\text{Tr}(\Phi^\dagger \Phi)]^2 + \lambda_5 \text{Tr}[(\Phi^\dagger \Phi)^2] + \lambda_6 [\text{Tr}(\tilde{\Phi} \tilde{\Phi}^*)]^2 + \lambda_7 \text{Tr}[(\tilde{\Phi} \tilde{\Phi}^*)^2] + \lambda_8(\chi_L^\dagger \chi_L) \text{Tr}(\Phi^\dagger \Phi) + \lambda_9(\chi_R^\dagger \chi_R) \text{Tr}(\Phi^\dagger \Phi) \\
 & + \lambda_{10}(\chi_L^\dagger \chi_L) \text{Tr}(\tilde{\Phi} \tilde{\Phi}^*) + \lambda_{11}(\chi_R^\dagger \chi_R) \text{Tr}(\tilde{\Phi} \tilde{\Phi}^*)
 \end{aligned} \quad (37)$$

where the term $\mu^2 \text{Tr}(\tilde{\Phi} \Phi^\dagger + \tilde{\Phi}^\dagger \Phi)$ softly breaks the $Z_4^{(1)}$ symmetry.

The minimization conditions of the scalar potential yields the following relations:

$$\mu_1^2 = \frac{1}{2} (-2\lambda_1 v_L^2 - \lambda_3 v_R^2 - (\lambda_8 + \lambda_{10}) v_1^2), \quad (38)$$

$$\mu_2^2 = \frac{1}{2} (-\lambda_3 v_L^2 - 2\lambda_2 v_R^2 - (\lambda_9 + \lambda_{11}) v_1^2), \quad (39)$$

$$\mu_3^2 = \frac{1}{2} (-(\lambda_8 + \lambda_{10}) v_L^2 - (\lambda_9 + \lambda_{11}) v_R^2 - 2(\lambda_4 + \lambda_5 + \lambda_6 + \lambda_7) v_1^2). \quad (40)$$

The squared mass matrix for the electrically charged scalars in the basis $(\chi_L^+, \chi_R^+, \phi_{1I}^+, \phi_{2I}^+) - (\chi_L^-, \chi_R^-, \phi_{1I}^-, \phi_{2I}^-)$ takes the form:

$$\mathbf{M}_{\text{charged}}^2 = \begin{pmatrix} 0 & 0 & 0 & 0 \\ 0 & 0 & 0 & 0 \\ 0 & 0 & \frac{1}{2} (-\lambda_{10} v_L^2 - \lambda_{11} v_R^2 - 2(\lambda_6 + \lambda_7) v_1^2) & -2\mu^2 \\ 0 & 0 & -2\mu^2 & \frac{1}{2} (-\lambda_{10} v_L^2 - \lambda_{11} v_R^2 - 2(\lambda_5 + \lambda_6 + \lambda_7) v_1^2) \end{pmatrix} \quad (41)$$

where the massless scalar eigenstates χ_L^\pm and χ_R^\pm correspond to the Goldstone bosons associated with the longitudinal components of the W^\pm and W'^\pm gauge bosons. Besides that, there are physical electrically charged scalars H_1^\pm and H_2^\pm , whose squared masses are given by:

$$m_{H_1^\pm}^2 = \frac{1}{2} \left(-\lambda_{10} v_L^2 - \lambda_{11} v_R^2 - \sqrt{16\mu^4 + \lambda_5^2 v_1^4} - \lambda_5 v_1^2 - 2\lambda_6 v_1^2 - 2\lambda_7 v_1^2 \right), \quad (42)$$

$$m_{H_2^\pm}^2 = \frac{1}{2} \left(-\lambda_{10} v_L^2 - \lambda_{11} v_R^2 + \sqrt{16\mu^4 + \lambda_5^2 v_1^4} - \lambda_5 v_1^2 - 2\lambda_6 v_1^2 - 2\lambda_7 v_1^2 \right). \quad (43)$$

The squared mass matrix for the CP-odd neutral scalar sector in the basis $(\text{Im } \chi_L^0, \text{Im } \chi_R^0, \phi_{1I}^0, \phi_{2I}^0)$

$$\mathbf{M}_{CP\text{-odd}}^2 = \begin{pmatrix} 0 & 0 & 0 & 0 \\ 0 & 0 & 0 & 0 \\ 0 & 0 & 0 & -2\mu^2 \\ 0 & 0 & -2\mu^2 & (\lambda_5 + \lambda_7)(-v_1^2) \end{pmatrix} \quad (44)$$

The massless scalar eigenstates $\text{Im } \chi_L^0$ and $\text{Im } \chi_R^0$ are associated with the Goldstone bosons associated with the longitudinal components of the Z and Z' gauge bosons. Furthermore, CP-odd neutral scalar sector contains two massive CP odd scalars whose squared masses are given by:

$$m_{A_1^0}^2 = \frac{1}{2} \left(-\sqrt{16\mu^4 + (\lambda_5 v_1^2 + \lambda_7 v_1^2)^2} - \lambda_5 v_1^2 - \lambda_7 v_1^2 \right), \quad (45)$$

$$m_{A_2^0}^2 = \frac{1}{2} \left(\sqrt{16\mu^4 + (\lambda_5 v_1^2 + \lambda_7 v_1^2)^2} - \lambda_5 v_1^2 - \lambda_7 v_1^2 \right). \quad (46)$$

The squared mass matrix for the CP-even neutral scalar sector in the basis $(\phi_{1R}^0, \text{Re } \chi_L^0, \phi_{2R}^0, \text{Re } \chi_R^0)$

$$\mathbf{M}_{CP\text{-even}}^2 = \begin{pmatrix} 2(\lambda_4 + \lambda_5 + \lambda_6 + \lambda_7)v_1^2 & (\lambda_8 + \lambda_{10})v_1 v_L & 2\mu^2 & (\lambda_9 + \lambda_{11})v_1 v_R \\ (\lambda_8 + \lambda_{10})v_1 v_L & 2\lambda_1 v_L^2 & 0 & \lambda_3 v_L v_R \\ 2\mu^2 & 0 & (\lambda_5 + \lambda_7)(-v_1^2) & 0 \\ (\lambda_9 + \lambda_{11})v_1 v_R & \lambda_3 v_L v_R & 0 & 2\lambda_2 v_R^2 \end{pmatrix} \quad (47)$$

Correlations between the masses of the non SM scalars are shown in Figure 4 and indicates that there are a large number of solutions for the scalar masses consistent with experimental bounds.

VI. HIGGS DIPHOTON DECAY RATE

The decay rate for the $h \rightarrow \gamma\gamma$ process takes the form:

$$\Gamma(h \rightarrow \gamma\gamma) = \frac{\alpha_{em}^2 m_h^3}{256\pi^3 v^2} \left| \sum_f a_{hff} N_C Q_f^2 F_{1/2}(\rho_f) + a_{hWW} F_1(\rho_W) + \sum_{k=1,2} \frac{C_{hH_k^\pm H_k^\mp} v}{2m_{H_k^\pm}^2} F_0(\rho_{H_k^\pm}) \right|^2, \quad (48)$$

where ρ_i are the mass ratios $\rho_i = \frac{m_h^2}{4M_i^2}$ with $M_i = m_f, M_W$; α_{em} is the fine structure constant; N_C is the color factor ($N_C = 1$ for leptons and $N_C = 3$ for quarks) and Q_f is the electric charge of the fermion in the loop. From the fermion-loop contributions we only consider the dominant top quark term. Furthermore, $C_{hH_k^\pm H_k^\mp}$ is the trilinear coupling between the SM-like Higgs and a pair of charged Higgses, whereas a_{htt} and a_{hWW} are the deviation factors from the SM Higgs-top quark coupling and the SM Higgs-W gauge boson coupling, respectively (in the SM these factors are unity). Such deviation factors are close to unity in our model, which is a consequence of the numerical analysis of its scalar, Yukawa and gauge sectors.

Furthermore, $F_{1/2}(z)$ and $F_1(z)$ are the dimensionless loop factors for spin-1/2 and spin-1 particles running in the internal lines of the loops. They are given by:

$$F_{1/2}(z) = 2(z + (z-1)f(z))z^{-2}, \quad (49)$$

$$F_1(z) = -2(2z^2 + 3z + 3(2z-1)f(z))z^{-2}, \quad (50)$$

$$F_0(z) = -(z - f(z))z^{-2}, \quad (51)$$

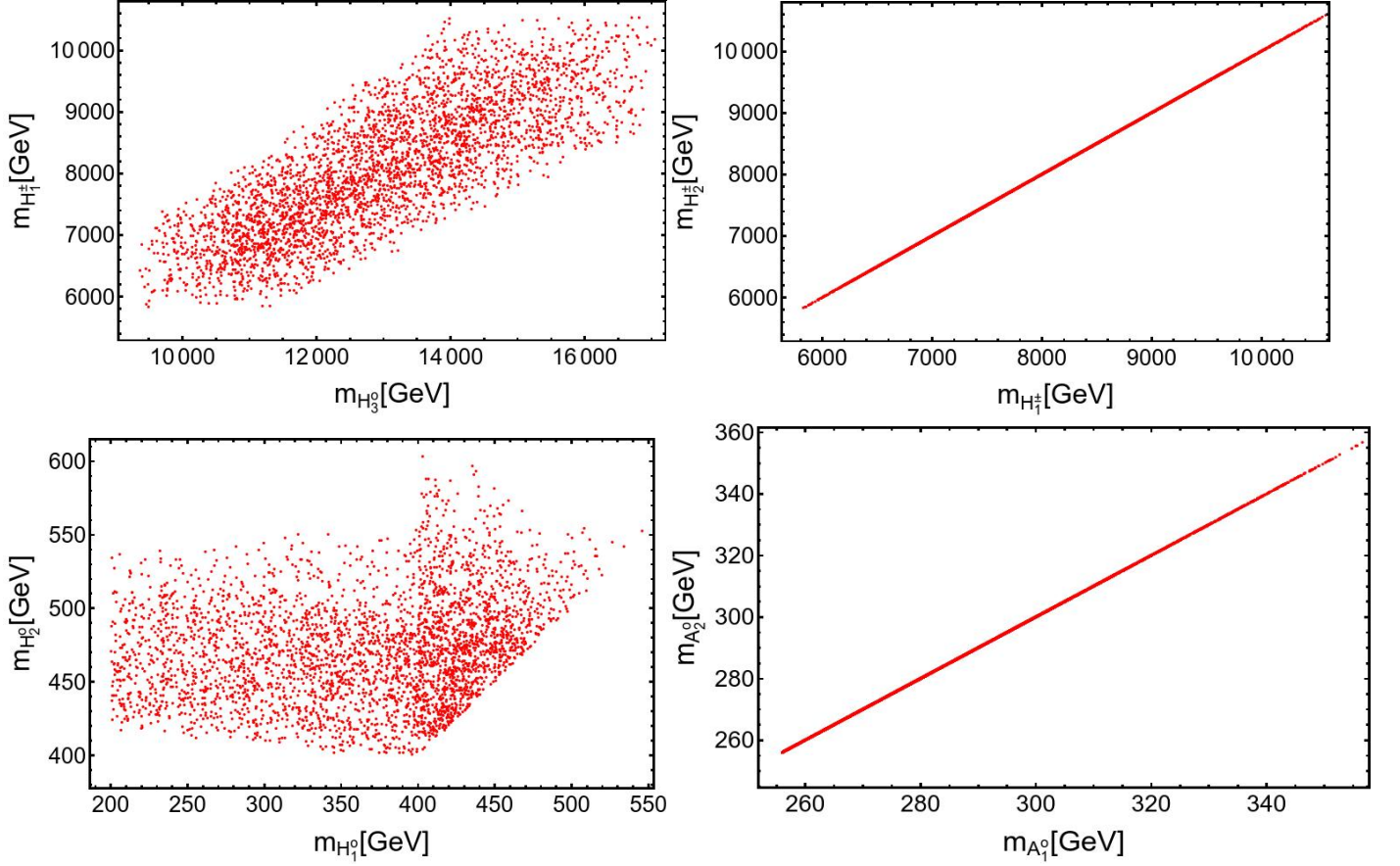


Figure 4: Correlations between the non SM scalar masses.

with

$$f(z) = \begin{cases} \arcsin^2 \sqrt{z} & \text{for } z \leq 1 \\ -\frac{1}{4} \left(\ln \left(\frac{1+\sqrt{1-z^{-1}}}{1-\sqrt{1-z^{-1}}-i\pi} \right)^2 \right) & \text{for } z > 1 \end{cases} \quad (52)$$

In order to study the implications of our model in the decay of the 126 GeV Higgs into a photon pair, one introduces the Higgs diphoton signal strength $R_{\gamma\gamma}$, which is defined as:

$$R_{\gamma\gamma} = \frac{\sigma(pp \rightarrow h)\Gamma(h \rightarrow \gamma\gamma)}{\sigma(pp \rightarrow h)_{SM}\Gamma(h \rightarrow \gamma\gamma)_{SM}} \simeq a_{htt}^2 \frac{\Gamma(h \rightarrow \gamma\gamma)}{\Gamma(h \rightarrow \gamma\gamma)_{SM}}. \quad (53)$$

That Higgs diphoton signal strength, normalizes the $\gamma\gamma$ signal predicted by our model in relation to the one given by the SM. Here we have used the fact that in our model, single Higgs production is also dominated by gluon fusion as in the Standard Model.

The ratio $R_{\gamma\gamma}$ has been measured by CMS and ATLAS collaborations with the best fit signals [18, 19]:

$$R_{\gamma\gamma}^{CMS} = 1.18^{+0.17}_{-0.14} \quad \text{and} \quad R_{\gamma\gamma}^{ATLAS} = 0.96 \pm 0.14. \quad (54)$$

The correlation of the Higgs diphoton signal strength with the charged scalar mass $m_{H_1^\pm}$ is shown in Figure 5, which indicates that our model successfully accommodates the current Higgs diphoton decay rate constraints. Furthermore, as indicated by Figure 5, our model favours a Higgs diphoton decay rate lower than the SM expectation but inside the 3σ experimentally allowed range.

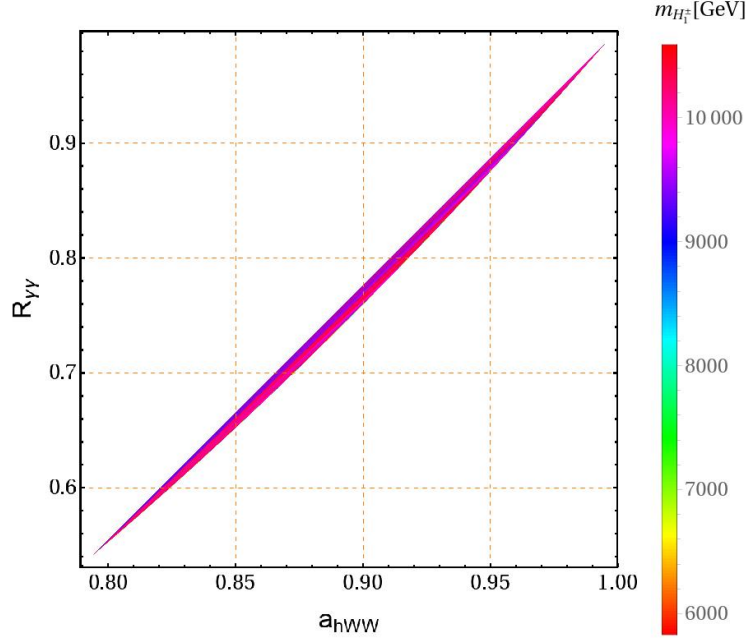


Figure 5: Correlation of the Higgs diphoton signal strength with the a_{hWW} deviation factor from the SM Higgs-W gauge boson coupling.

VII. MUON AND ELECTRON ANOMALOUS MAGNETIC MOMENTS

In this section we will analyze the implications of our model in the muon and electron anomalous magnetic moments. The leading contributions of the muon and electron anomalous magnetic moments arise from vertex diagrams involving the exchange of neutral scalars and vector like leptons running in the internal lines of the loop. Then, in our model the contributions to the muon and electron anomalous magnetic moments take the form:

$$\begin{aligned} \Delta a_\mu &= \sum_{k=1}^2 \frac{\beta_{2k} \gamma_{k2} m_\mu^2}{8\pi^2} \left[(R_{CP\text{-even}}^T)_{21} (R_{CP\text{-even}}^T)_{41} I_S^{(\mu)}(m_{E_k}, m_{h^0}) + \sum_{i=1}^3 (R_{CP\text{-even}}^T)_{2i} (R_{CP\text{-even}}^T)_{4i} I_S^{(\mu)}(m_{E_k}, m_{H_i^0}) \right], \\ \Delta a_e &= \sum_{k=1}^2 \frac{\beta_{1k} \gamma_{k1} m_e^2}{8\pi^2} \left[(R_{CP\text{-even}}^T)_{21} (R_{CP\text{-even}}^T)_{41} I_S^{(e)}(m_{E_k}, m_{h^0}) + \sum_{i=1}^3 (R_{CP\text{-even}}^T)_{2i} (R_{CP\text{-even}}^T)_{4i} I_S^{(e)}(m_{E_k}, m_{H_i^0}) \right], \end{aligned} \quad (55)$$

where the loop $I_{S(P)}(m_E, m)$ has the form [20–22]:

$$I_{S(P)}^{(e,\mu)}(m_E, m_S) = \int_0^1 \frac{x^2 \left(1 - x \pm \frac{m_E}{m_{e,\mu}}\right)}{m_\mu^2 x^2 + (m_E^2 - m_{e,\mu}^2)x + m_{S,P}^2(1-x)} dx \quad (56)$$

Considering that the muon and electron anomalous magnetic moments are constrained to be in the ranges [23–25]:

$$\begin{aligned} (\Delta a_\mu)_{\text{exp}} &= (26.1 \pm 8) \times 10^{-10} \\ (\Delta a_e)_{\text{exp}} &= (-0.88 \pm 0.36) \times 10^{-12}. \end{aligned} \quad (57)$$

We plot in Figure 6 the correlations of the muon and electron anomalous magnetic moments with the mass m_{E_1} of one of the charged exotic leptons (top plots) as well as the correlation between the electron and muon anomalous magnetic moments (bottom plot), for fixed values of the CP even neutral scalar masses. We have checked that the

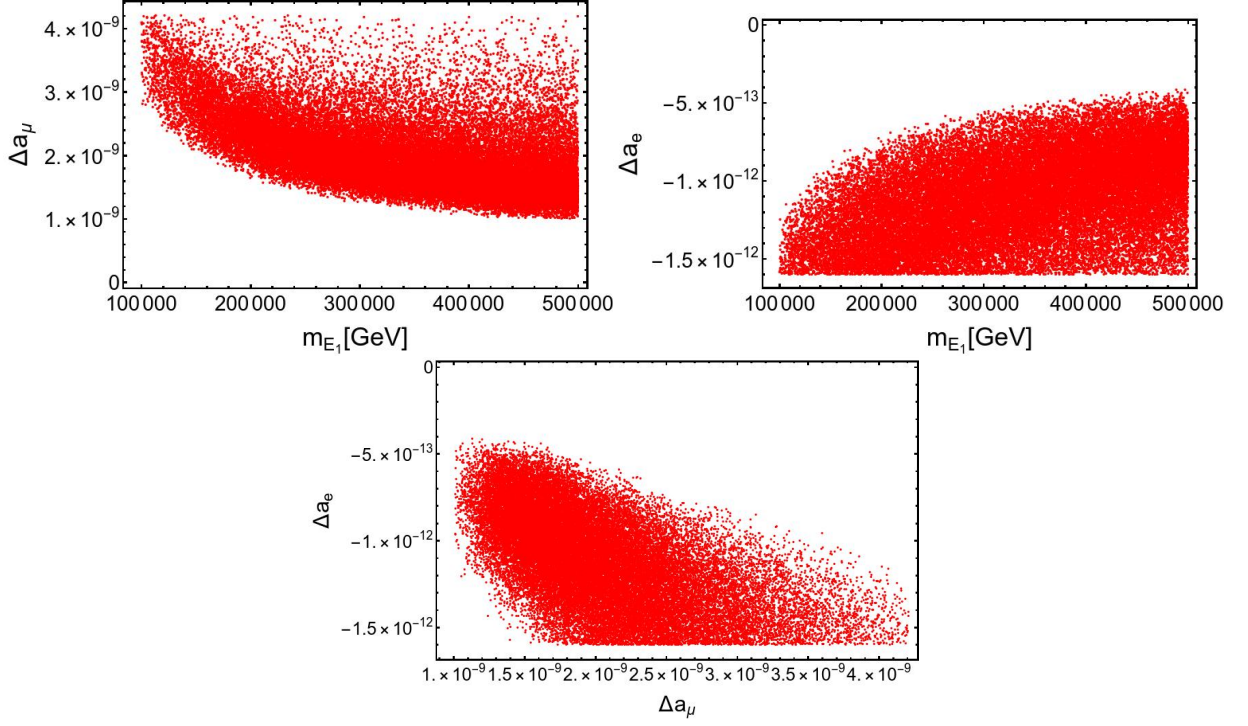


Figure 6: Correlations of the muon and electron anomalous magnetic moments with the mass m_{E_1} of one of the charged exotic leptons (top plots). Correlation between the electron and muon anomalous magnetic moments (bottom plot).

correlations of $\Delta a_{\mu,e}$ with m_{E_2} are very similar with the ones involving m_{E_1} instead of m_{E_2} . Here we have fixed $m_{H_1^0} = 400$ GeV, $m_{H_2^0} = 500$ GeV and $m_{H_3^0} = 12$ TeV. We find that our model can successfully accommodate the experimental values of the muon and electron anomalous magnetic moments.

VIII. HEAVY SCALAR PRODUCTION AT THE LHC

In this section we discuss the singly heavy scalar H_1^0 production at a proton-proton collider. Such production mechanism at the LHC is dominated by the gluon fusion mechanism, which is a one-loop process mediated by the top quark. Thus, the total H_1^0 production cross section in proton-proton collisions with center of mass energy \sqrt{S} takes the form:

$$\sigma_{pp \rightarrow gg \rightarrow H_1^0}(S) = \frac{\alpha_S^2 a_{H_1^0 t \bar{t}}^2 m_{H_1^0}^2}{64\pi v^2 S} \left[I\left(\frac{m_{H_1^0}^2}{m_t^2}\right) \right]^2 \int_{\ln \sqrt{\frac{m_{H_1^0}^2}{S}}}^{-\ln \sqrt{\frac{m_{H_1^0}^2}{S}}} f_{p/g} \left(\sqrt{\frac{m_{H_1^0}^2}{S}} e^y, \mu^2 \right) f_{p/g} \left(\sqrt{\frac{m_{H_1^0}^2}{S}} e^{-y}, \mu^2 \right) dy, \quad (58)$$

where $f_{p/g}(x_1, \mu^2)$ and $f_{p/g}(x_2, \mu^2)$ are the distributions of gluons in the proton which carry momentum fractions x_1 and x_2 of the proton, respectively. Furthermore $\mu = m_{H_1}$ is the factorization scale, whereas $I(z)$ has the form:

$$I(z) = \int_0^1 dx \int_0^{1-x} dy \frac{1-4xy}{1-zxy}. \quad (59)$$

Figure 7 shows the H_1^0 total production cross section at the LHC via gluon fusion mechanism for $\sqrt{S} = 14$ TeV (left-plot) and $\sqrt{S} = 28$ TeV (right-plot), as a function of the scalar mass $m_{H_1^0}$, which is taken to range from 400 GeV up to 600 GeV. Furthermore, the coupling $a_{H_1^0 t \bar{t}}$ of the heavy scalar H_1^0 with the top-antitop quark pair has been set to be equal to 0.4, which is consistent with our numerical analysis of the scalar potential. In the aforementioned

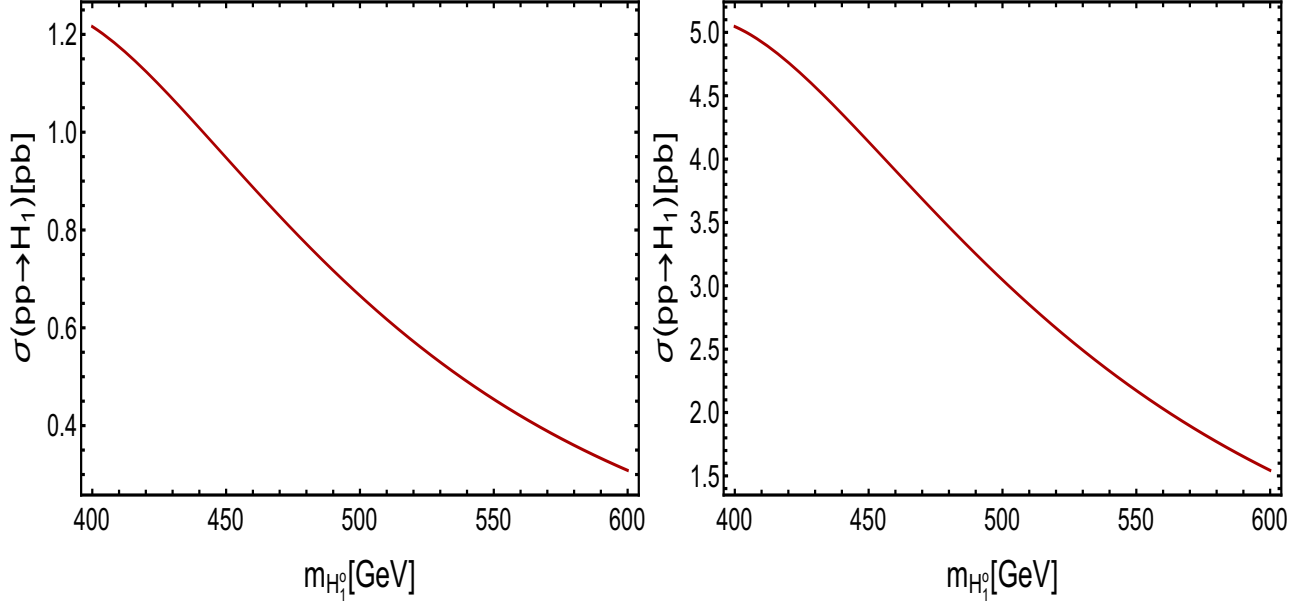


Figure 7: Total cross section for the H_1^0 production via gluon fusion mechanism at the LHC for $\sqrt{s} = 14$ TeV (left-panel) and $\sqrt{s} = 28$ (right-panel) TeV as a function of the heavy scalar mass $m_{H_1^0}$.

region of masses for the heavy H_1 scalar, we find that the total production cross section ranges from 1.2 pb up to 0.3 pb. However, at the proposed energy upgrade of the LHC with $\sqrt{s} = 28$ TeV, the total cross section for the H_1^0 is enhanced reaching values between 5 pb and 1.5 pb in the aforementioned mass range as indicated in the right panel of Figure 7. The heavy neutral H_1^0 scalar, after being produced, will have dominant decay modes into top-antitop quark pairs, SM Higgs boson pairs as well as into a pair of SM gauge bosons, thus implying that the observation of an excess of events in the multileptons or multijet final states over the SM background can be a smoking gun signature of this model, whose observation will be crucial to assess its viability.

IX. Z' GAUGE BOSON PRODUCTION AT THE LHC

In this section we discuss the single heavy Z' gauge boson via Drell-Yan mechanism at proton-proton collider. We consider the dominant contributions due to the parton distribution functions of the light up, down and strange quarks, so that the total cross section for the production of a Z' via quark antiquark annihilation in proton-proton collisions with center of mass energy \sqrt{S} takes the form:

$$\sigma_{pp \rightarrow Z'}^{(DrellYan)}(S) = \frac{g_R^2 \pi}{24S} \int_{\ln \sqrt{\frac{m_{Z'}^2}{S}}}^{-\ln \sqrt{\frac{m_{Z'}^2}{S}}} \sum_{q=u,d,s} f_{p/q} \left(\sqrt{\frac{m_{Z'}^2}{S}} e^y, \mu^2 \right) f_{p/\bar{q}} \left(\sqrt{\frac{m_{Z'}^2}{S}} e^{-y}, \mu^2 \right) dy \quad (60)$$

where $f_{p/u}(x_1, \mu^2)$ ($f_{p/\bar{u}}(x_2, \mu^2)$), $f_{p/d}(x_1, \mu^2)$ ($f_{p/\bar{d}}(x_2, \mu^2)$) and $f_{p/s}(x_1, \mu^2)$ ($f_{p/\bar{s}}(x_2, \mu^2)$) are the distributions of the light up, down and strange quarks (antiquarks), respectively, in the proton which carry momentum fractions x_1 (x_2) of the proton. The factorization scale is taken to be $\mu = m_{Z'}$. Fig. 8 displays the Z' total production cross section at the LHC via the Drell-Yan mechanism for $\sqrt{S} = 14$ TeV (left panel) and $\sqrt{S} = 28$ TeV (right panel) as a function of the Z' mass $M_{Z'}$ in the range from 4 TeV up to 5 TeV. For this region of Z' masses we find that the total production cross section ranges from 13 fb up to 1 fb. The heavy neutral Z' gauge boson, after being produced, will subsequently decay into the pair of the SM fermion-antifermion pairs, thus implying that the observation of an excess of events in the dileptons or dijet final states over the SM background can be a signal of support of this model at the LHC. On the other hand, at the proposed energy upgrade of the LHC at 28 TeV center of mass energy, the total cross

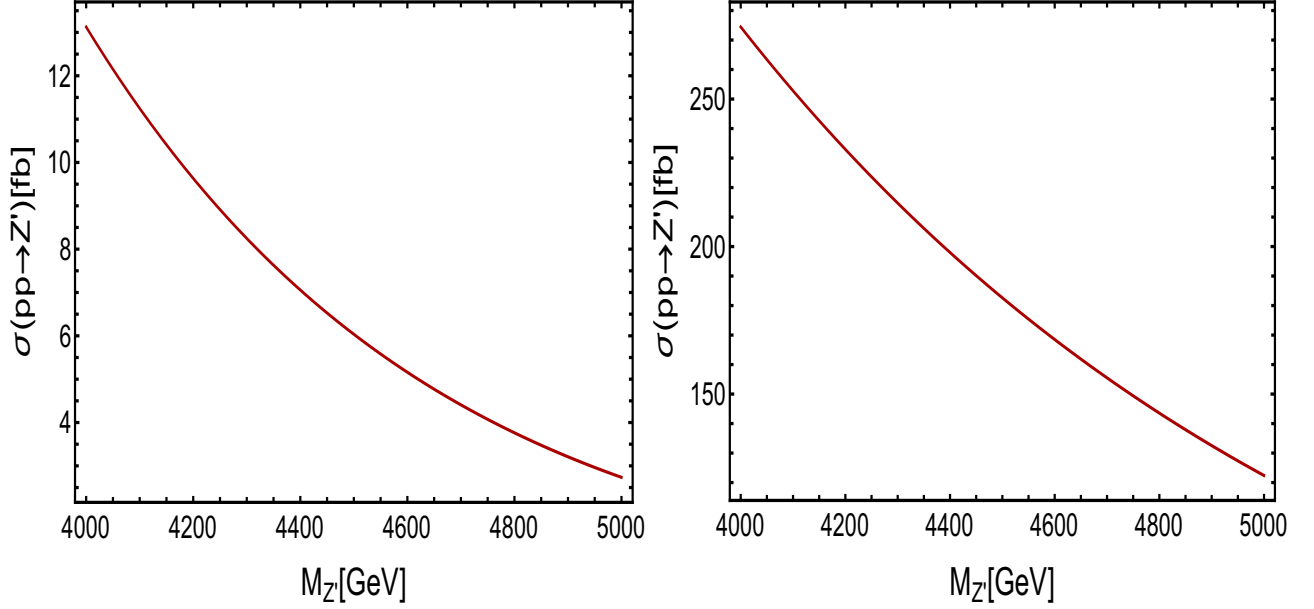


Figure 8: Total cross section for the Z' production via Drell-Yan mechanism at a proton-proton collider for $\sqrt{S} = 14$ TeV (left-panel) and $\sqrt{S} = 28$ (right-panel) TeV as a function of the Z' mass.

section for the Drell-Yan production of a heavy Z' neutral gauge boson gets significantly enhanced reaching values ranging from 280 fb up to 120 fb, as indicated in the right panel of Fig. 8.

X. CONCLUSIONS

We have built a renormalizable left-right symmetric theory with additional symmetry $Z_4^{(1)} \times Z_4^{(2)}$ consistent with the observed SM fermion mass hierarchy, the tiny values for the light active neutrino masses, the lepton and baryon asymmetries of the Universe as well as the muon and electron anomalous magnetic moments. As the main appealing feature of the proposed model, the top and exotic fermions get their masses at tree level whereas the masses of the bottom, charm and strange quarks, tau and muon leptons are generated from a tree level Universal Seesaw mechanism thanks to their mixings with charged exotic vector like fermions. The first generation SM charged fermions masses are produced from a radiative seesaw mechanism at one loop level mediated by charged vector like fermions and electrically neutral scalars. The tiny masses of the light active neutrinos arise from an inverse seesaw mechanism at one-loop level. Furthermore, we have also shown that the proposed model successfully accommodates the current Higgs diphoton decay rate constraints, yielding a Higgs diphoton decay rate lower than the SM expectation but inside the 3σ experimentally allowed range. We also studied the heavy H_1^0 scalar and Z' gauge boson production in a proton-proton collider at $\sqrt{S} = 14$ TeV and $\sqrt{S} = 28$ TeV, via the gluon fusion and Drell-Yan mechanisms, respectively. We found that the singly H_1^0 scalar production cross section reach values of 1.2 and 5 pb at $\sqrt{S} = 14$ TeV and $\sqrt{S} = 28$ TeV, respectively, for a 400 GeV heavy scalar mass. On the other hand, we found that the total cross section for the Z' gauge boson production takes the values of 13 fb and 280 fb at $\sqrt{S} = 14$ TeV and $\sqrt{S} = 28$ TeV, respectively, for a 4 TeV Z' gauge boson mass.

Acknowledgments

A.E.C.H and I.S. are supported by ANID-Chile FONDECYT 1170803, ANID-Chile FONDECYT 1180232 and ANID-Chile FONDECYT 3150472, and by the project ANID PIA/APOYO AFB180002 (Chile)

-
- [1] J. C. Pati and A. Salam, “Lepton Number as the Fourth Color,” *Phys. Rev.* **D10** (1974) 275–289. [Erratum: *Phys. Rev.* **D11**, 703(1975)].
 - [2] R. N. Mohapatra and J. C. Pati, “A Natural Left-Right Symmetry,” *Phys. Rev.* **D11** (1975) 2558.
 - [3] A. E. Cárcamo Hernández, S. Kovalenko, J. W. F. Valle, and C. A. Vaquera-Araujo, “Neutrino predictions from a left-right symmetric flavored extension of the standard model,” *JHEP* **02** (2019) 065, [arXiv:1811.03018 \[hep-ph\]](#).
 - [4] W. Dekens and D. Boer, “Viability of minimal left–right models with discrete symmetries,” *Nucl. Phys.* **B889** (2014) 727–756, [arXiv:1409.4052 \[hep-ph\]](#).
 - [5] E. Ma, “Universal Scotogenic Fermion Masses in Left-Right Gauge Model,” [arXiv:2012.03128 \[hep-ph\]](#).
 - [6] K. Babu and A. Thapa, “Left-Right Symmetric Model without Higgs Triplets,” [arXiv:2012.13420 \[hep-ph\]](#).
 - [7] M. Escudero, A. Berlin, D. Hooper, and M.-X. Lin, “Toward (Finally!) Ruling Out Z and Higgs Mediated Dark Matter Models,” *JCAP* **1612** (2016) 029, [arXiv:1609.09079 \[hep-ph\]](#).
 - [8] N. Bernal, A. E. Cárcamo Hernández, I. de Medeiros Varzielas, and S. Kovalenko, “Fermion masses and mixings and dark matter constraints in a model with radiative seesaw mechanism,” *JHEP* **05** (2018) 053, [arXiv:1712.02792 \[hep-ph\]](#).
 - [9] A. E. Cárcamo Hernández, J. W. F. Valle, and C. A. Vaquera-Araujo, “Simple theory for scotogenic dark matter with residual matter-parity,” *Phys. Lett.* **B809** (2020) 135757, [arXiv:2006.06009 \[hep-ph\]](#).
 - [10] Z.-L. Han and W. Wang, “Predictive Scotogenic Model with Flavor Dependent Symmetry,” *Eur. Phys. J.* **C79** no. 6, (2019) 522, [arXiv:1901.07798 \[hep-ph\]](#).
 - [11] M. E. Cabrera, J. A. Casas, A. Delgado, and S. Robles, “2HDM singlet portal to dark matter,” [arXiv:2011.09101 \[hep-ph\]](#).
 - [12] M. E. Catano, R. Martinez, and F. Ochoa, “Neutrino masses in a 331 model with right-handed neutrinos without doubly charged Higgs bosons via inverse and double seesaw mechanisms,” *Phys. Rev.* **D86** (2012) 073015, [arXiv:1206.1966 \[hep-ph\]](#).
 - [13] P.-H. Gu and U. Sarkar, “Leptogenesis with Linear, Inverse or Double Seesaw,” *Phys. Lett.* **B694** (2011) 226–232, [arXiv:1007.2323 \[hep-ph\]](#).
 - [14] A. Pilaftsis, “CP violation and baryogenesis due to heavy Majorana neutrinos,” *Phys. Rev.* **D56** (1997) 5431–5451, [arXiv:hep-ph/9707235 \[hep-ph\]](#).
 - [15] M. J. Dolan, T. P. Dutka, and R. R. Volkas, “Dirac-Phase Thermal Leptogenesis in the extended Type-I Seesaw Model,” *JCAP* **1806** (2018) 012, [arXiv:1802.08373 \[hep-ph\]](#).
 - [16] S. Blanchet, T. Hambye, and F.-X. Josse-Michaux, “Reconciling leptogenesis with observable $\mu \rightarrow e \gamma$ rates,” *JHEP* **04** (2010) 023, [arXiv:0912.3153 \[hep-ph\]](#).
 - [17] W. Grimus and L. Lavoura, “The Seesaw mechanism at arbitrary order: Disentangling the small scale from the large scale,” *JHEP* **11** (2000) 042, [arXiv:hep-ph/0008179 \[hep-ph\]](#).
 - [18] CMS Collaboration, A. M. Sirunyan *et al.*, “Measurements of Higgs boson properties in the diphoton decay channel in proton-proton collisions at $\sqrt{s} = 13$ TeV,” *JHEP* **11** (2018) 185, [arXiv:1804.02716 \[hep-ex\]](#).
 - [19] ATLAS Collaboration, G. Aad *et al.*, “Combined measurements of Higgs boson production and decay using up to 80 fb⁻¹ of proton-proton collision data at $\sqrt{s} = 13$ TeV collected with the ATLAS experiment,” *Phys. Rev.* **D101** no. 1, (2020) 012002, [arXiv:1909.02845 \[hep-ex\]](#).
 - [20] R. A. Diaz, R. Martinez, and J. A. Rodriguez, “Phenomenology of lepton flavor violation in 2HDM(3) from (g-2)(mu) and leptonic decays,” *Phys. Rev.* **D67** (2003) 075011, [arXiv:hep-ph/0208117 \[hep-ph\]](#).
 - [21] C. Kelso, H. N. Long, R. Martinez, and F. S. Queiroz, “Connection of $g - 2_\mu$, electroweak, dark matter, and collider constraints on 331 models,” *Phys. Rev.* **D90** no. 11, (2014) 113011, [arXiv:1408.6203 \[hep-ph\]](#).
 - [22] K. Kowalska and E. M. Sessolo, “Expectations for the muon g-2 in simplified models with dark matter,” *JHEP* **09** (2017) 112, [arXiv:1707.00753 \[hep-ph\]](#).
 - [23] K. Hagiwara, R. Liao, A. D. Martin, D. Nomura, and T. Teubner, “ $(g - 2)_\mu$ and $\alpha(M_Z^2)$ re-evaluated using new precise

- data,” *J. Phys.* **G38** (2011) 085003, [arXiv:1105.3149 \[hep-ph\]](#).
- [24] T. Nomura and H. Okada, “One-loop neutrino mass model without any additional symmetries,” *Phys. Dark Univ.* **26** (2019) 100359, [arXiv:1808.05476 \[hep-ph\]](#).
- [25] T. Nomura and H. Okada, “Zee-Babu type model with $U(1)_{L_\mu-L_\tau}$ gauge symmetry,” *Phys. Rev.* **D97** no. 9, (2018) 095023, [arXiv:1803.04795 \[hep-ph\]](#).